SPACE SCIENCE AND GEOSPATIAL INSTITUTE
FROM EARTH TO SPACE . . .

Ionospheric response to the 23-31 August 2018 Geomagnetic storm in the Europe-African longitude sector using multi-instrument observations

Teshome Dugassa[a], Nigussie Mezgebe[a], John Bosco Habarulema[b,c], Valence Habyarimana[d], Asebe Oljira[e]

[a] Space Science and Geospatial Institute, Addis Ababa, Ethiopia
[b] South Africa National Space Agency, Space Science, Hermanus, South Africa
[c] Department of Physics and Electronics, Rhodes University, Grahamstown, South Africa
[d] Department of Physics, Mbarara University of Science and Technology, Mbarara, Uganda
[e] Department of Physics, Wollega University, Nekemete, Ethiopia

United Nations Workshop on the International Space Weather Initiative:The Way Forward, 26-30 June 2023
Vienna, Austria

Outlines

- **Background**
- **Motivation**
- **Data and Method of analysis**
- **Result: Ionospheric response & Ionospheric irregularities**
- **Conclusion**

Background: Geomagnetic storm

- The geomagnetic storms (GMS) is a disturbance in Earth's B-field; developed when large quantities of disturbed solar wind plasma interact with Earth's B-field.
- Based on their driving sources, geomagnetic storms can be classified as due to
  - Coronal Mass Ejections (CMEs)
  - Corotating Interaction Regions (CIRs)

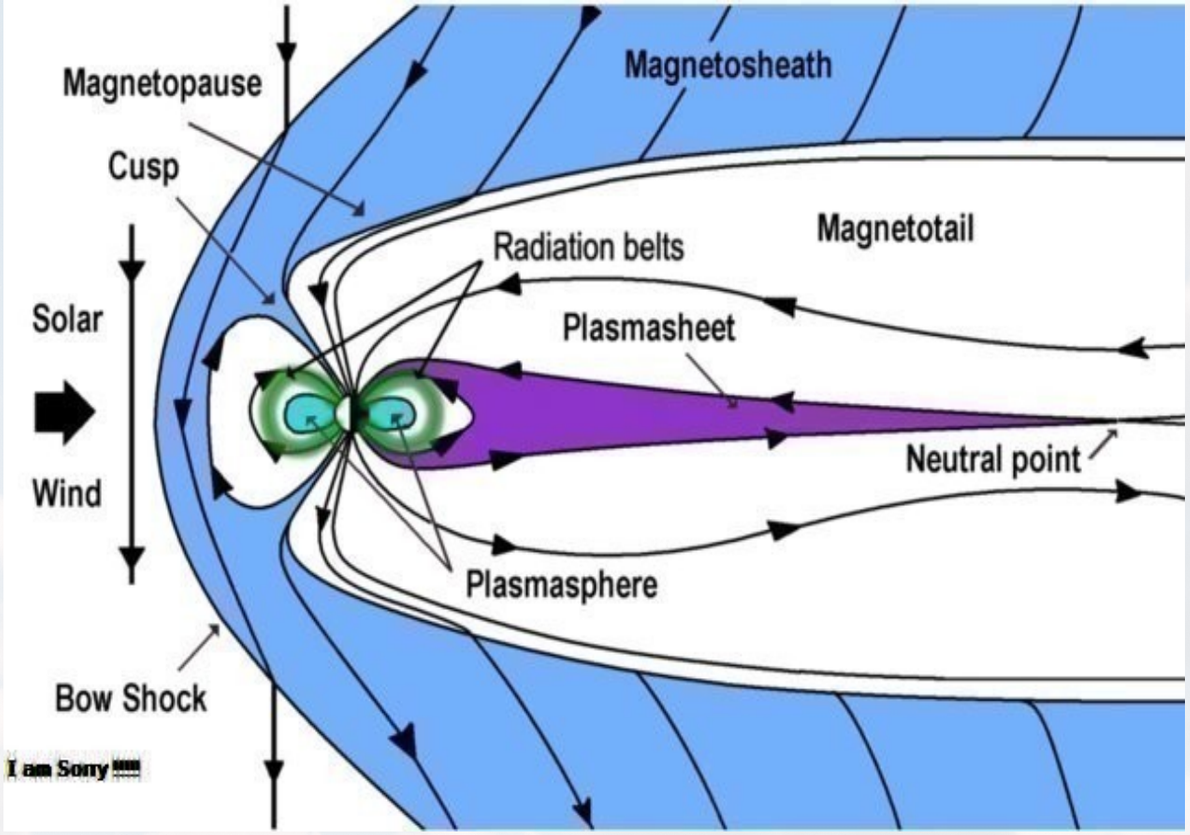

- Their geoeffectiveness depends primarily on a sustained orientation of IMFBz (southward orientation).
  - Large amount of solar wind energy deposit into Earth's magnetosphere
- Leads to a series of storm-time processes that greatly modify the dynamics of the thermosphere and ionosphere.

Background: Ionospheric Storms

- Ionospheric storms: Perturbations in the ionosphere during GMSs; the ionospheric parameters significantly changes from its quiet time values.
- The major responses
  - Positive and
  - Negative ionospheric storm

- The response of the ionosphere to a specific GMS depends on its
  - Onset time of the storm,
  - Season (equinox, solstice),
  - solar activity (high, low),
  - Drivers of the storm (CME, CIR)
  - Geographic/Geomagnetic location

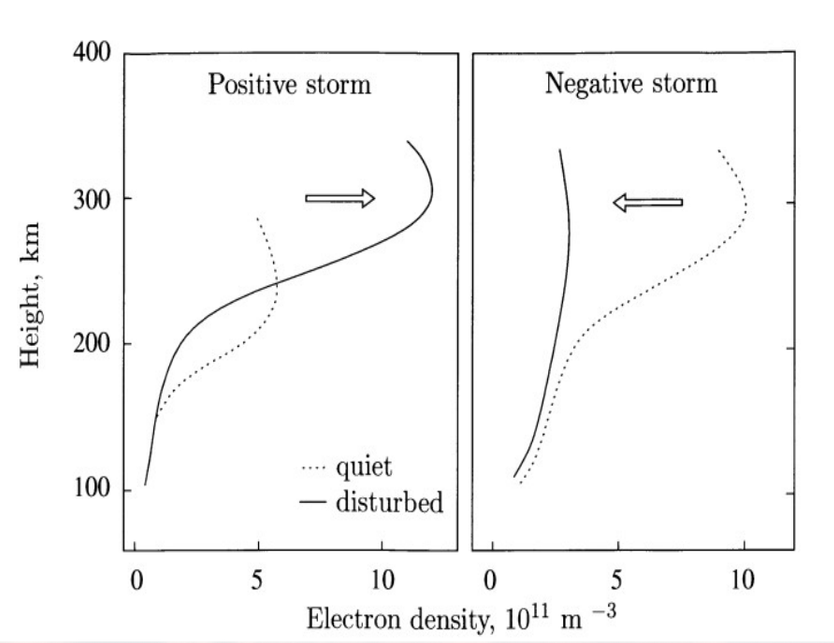

August 2018 Space Weather Event

- On the approach to minimum of Solar Cycle 24, on 26 August 2018, an **unexpectedly strong GMS (G3) suddenly occurred**.
- Such a strong G3 GMS was not foreseen by forecasters.
- According to the NOAA Space Weather Prediction Center (SWPC) a minor G1 GMS was expected.
- The 25-26 August 2018 storm event was classified as the 3rd largest geomagnetic storm of the 24th solar cycle after the March 2015 and June 2015 geomagnetic storms.
- Images of the filaments, coronal holes, and the CMEs that caused the August 26, 2018 geomagnetic storm.

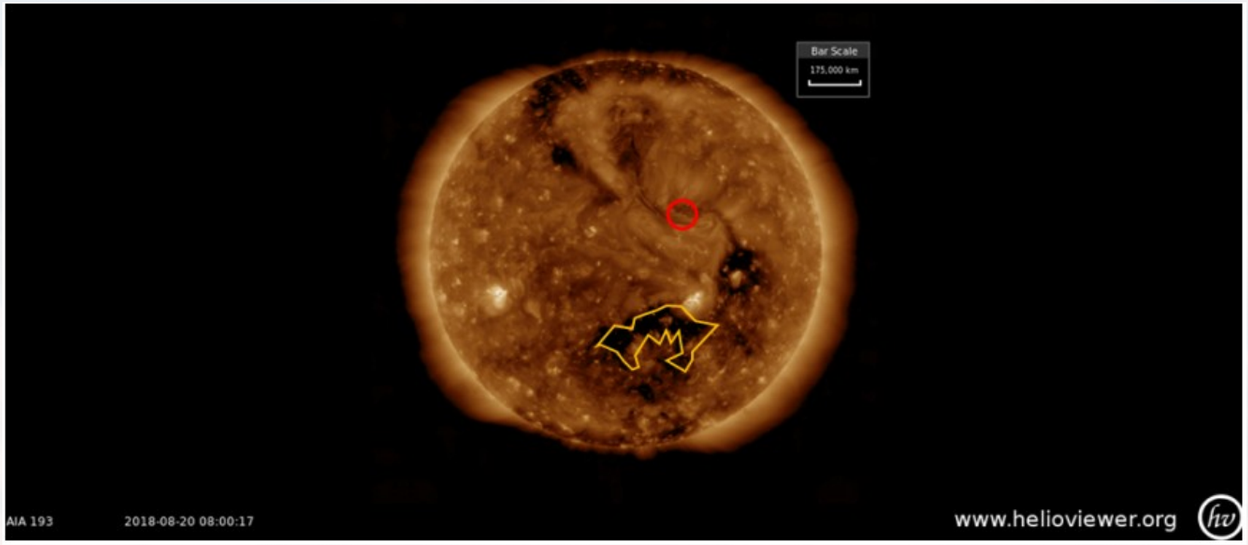

https://helioviewer.org/

- The storm were caused by a **non-AR central filament** two-step eruption on 20 August which was accompanied by two consecutive Earth-directed low-speed CMEs.

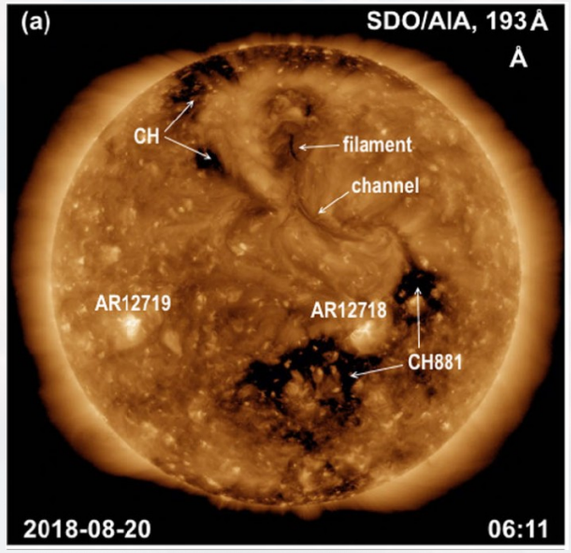

The SDO/AIA 193 Å images before the eruptions (Abunin et al., 2020)

Motivation

- The space weather events of such intensity occurring during the solar minimum period and at the background of the very low ionospheric density can result in a strong ionosphere-thermosphere response.
- Previous papers were devoted on the investigation of the positive and negative ionospheric storm effects on the ionospheric density distribution over the globe (Astafyeva et al., 2020; Mansilla and Zossi, 2020; Younas et al., 2020), as well as regional effects in Asia (Lissa et al., 2020) and over Brazil (Spogli et al., 2021), and reported inter-hemispheric asymmetries of the ionospheric response during this event.
- Another crucial aspect of the Earth's ionosphere response is generation of different scale ionospheric irregularities driven by geomagnetic storm development.
- Despite numbers of investigations during the storm event were made over different longitude and latitude sectors, we realize that there is still scope in understanding of the driving mechanisms and possible effects on a regional aspect, in particular, for the European-African longitude sector.

Data and Method of analysis

Data sources

- Global Navigation Satellite System (GNSS)
- Global Ionospheric Maps (GIMs)
- In-situ electron density (Ne)
  - SWARM satellite
  - DMSP satellite
- Thermospheric [O]/[N_2] composition
- Prompt Penetration Electric Field Model
- Solar wind and geomagnetic parameters

ftp:cddis.nasa.gov/gnss/data
ftp://cddis.gfsc.nasa.gov/pub/gps/products/ionex
http://earth.esa.int/swarm or http://vires.services
http://cedar.openmadrigal.org
http://guvitimed.jhuapl.edu/data_on2_info
https://geomag.org/models/PPEFM/RealtimeEF.html
https://cdaweb.gsfc.nasa.gov/index.html

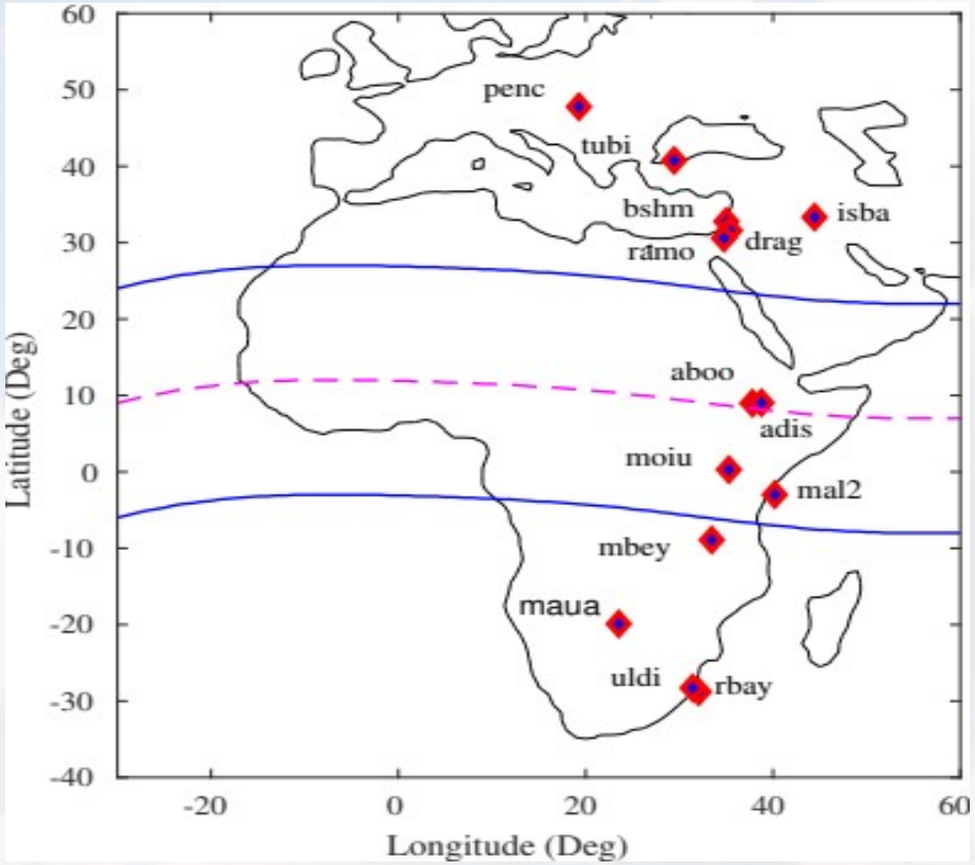

Figure 2: Map showing the geographic coordinates of the stations used in the study. The the magenta broken curve and blue solid curves shows the magnetic dip equator and off magnetic equator at about ±15°. The region between the solid blue lines show the low-latitude region.

Data and Method of analysis

$$VTEC = \frac{STEC - (b_R + b_S)}{M(\phi)}$$

$$M(\phi) = \frac{1}{\cos\theta} = \left[1 - \left(\frac{R_E \cos(\phi)}{R_E + h}\right)^2\right]^{-1/2}$$

$$\Delta TEC = \frac{TEC_{obs} - TEC_m}{TEC_m} \times 100\%$$

GPS-TEC
Ionospheric perturbation
GIM-TEC

$$\Delta VTEC_{lat,lon,LT,day} = VTEC_{lat,lon,LT,day} - VTEC_{lat,lon,LT,day-1}$$

Index for ionospheric irregularities

From Ground based GPS observation

$$ROTI = \sqrt{\langle ROT^2 \rangle - \langle ROT \rangle^2}$$

$$ROT = \frac{dTEC}{dt} = \frac{TEC(t_{i+1}) - TEC(t_i)}{t_{i+1} - t_i}$$

From in-situ measurement by SWARM-A, B satellites

$$RODI = \sqrt{\langle ROD^2 \rangle - \langle ROD \rangle^2}$$

$$ROD = \frac{N_e(t + \Delta t) - N_e(t)}{\Delta t}$$

Geophysical condition of the 23-31 August 2018 storm

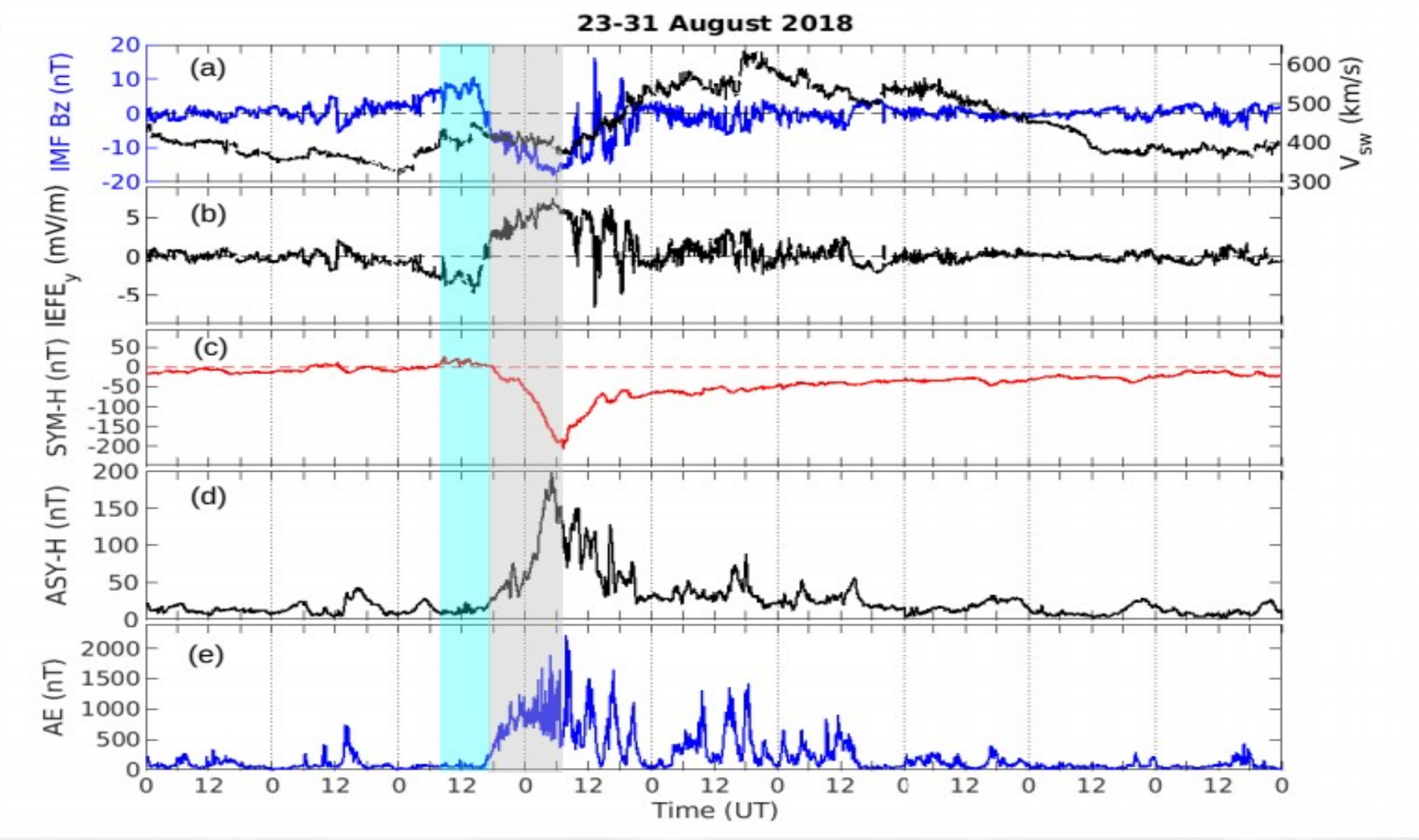

Figure 1: Temporal variation of the solar wind parameters and geomagnetic index. (a) the z-component of interplanetary magnetic field (IMF Bz, blue) and the solar wind speed (V sw, black), (b) the y-component of interplanetary electric field (IEEy), (c) the symmetric ring current (SYM-H), (d) asymmetric ring current (ASY-H) and (e) Auroral electrojet (AE) during 23-31 August 2018 period. The light cyan and the gray shaded regions show the initial and main phase of the storm, respectively (Dugassa et al., 2022).

Ionospheric response: ΔTEC from GIM

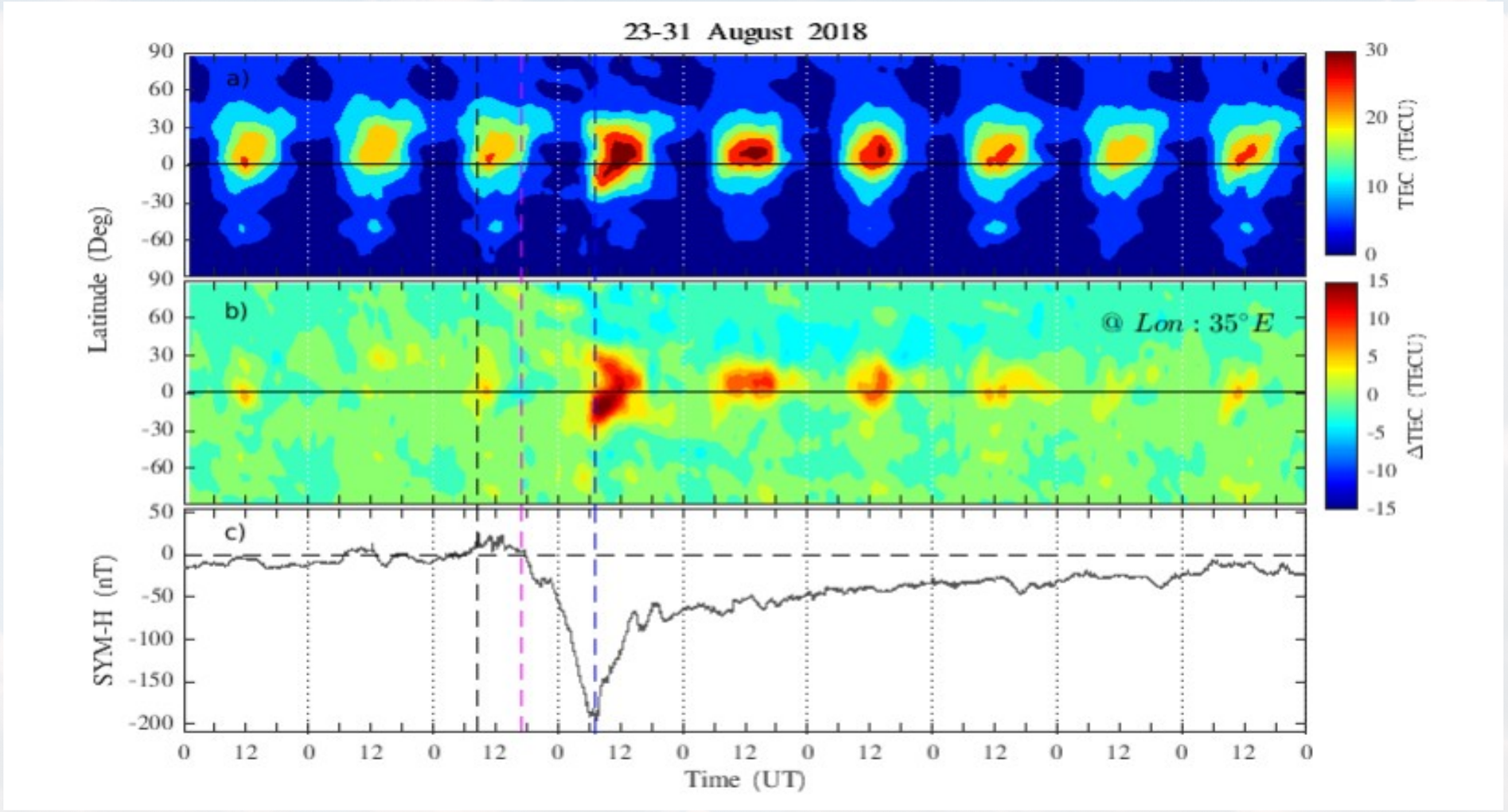

Figure 3: Variation in (a) ionospheric TEC (b) DTEC (in TECU) derived from GIM over Europe-African longitude sector (along 35°E). The **solid gray line shows the magnetic dip equator** during 23 August 2018; (c) the geomagnetic index (SYM-H) during 23-31 August 2018 storm period. **The vertical broken gray, magenta, and blue lines show the beginning of the initial** (07:45 UT, 25 August 2018), **main** (17:29 UT, 25 August 2018), and **recovery** (07:00 UT, 26 August 2018) phases of the storm, respectively (Dugassa et al., 2022).

Ionospheric response: ΔTEC from GIM

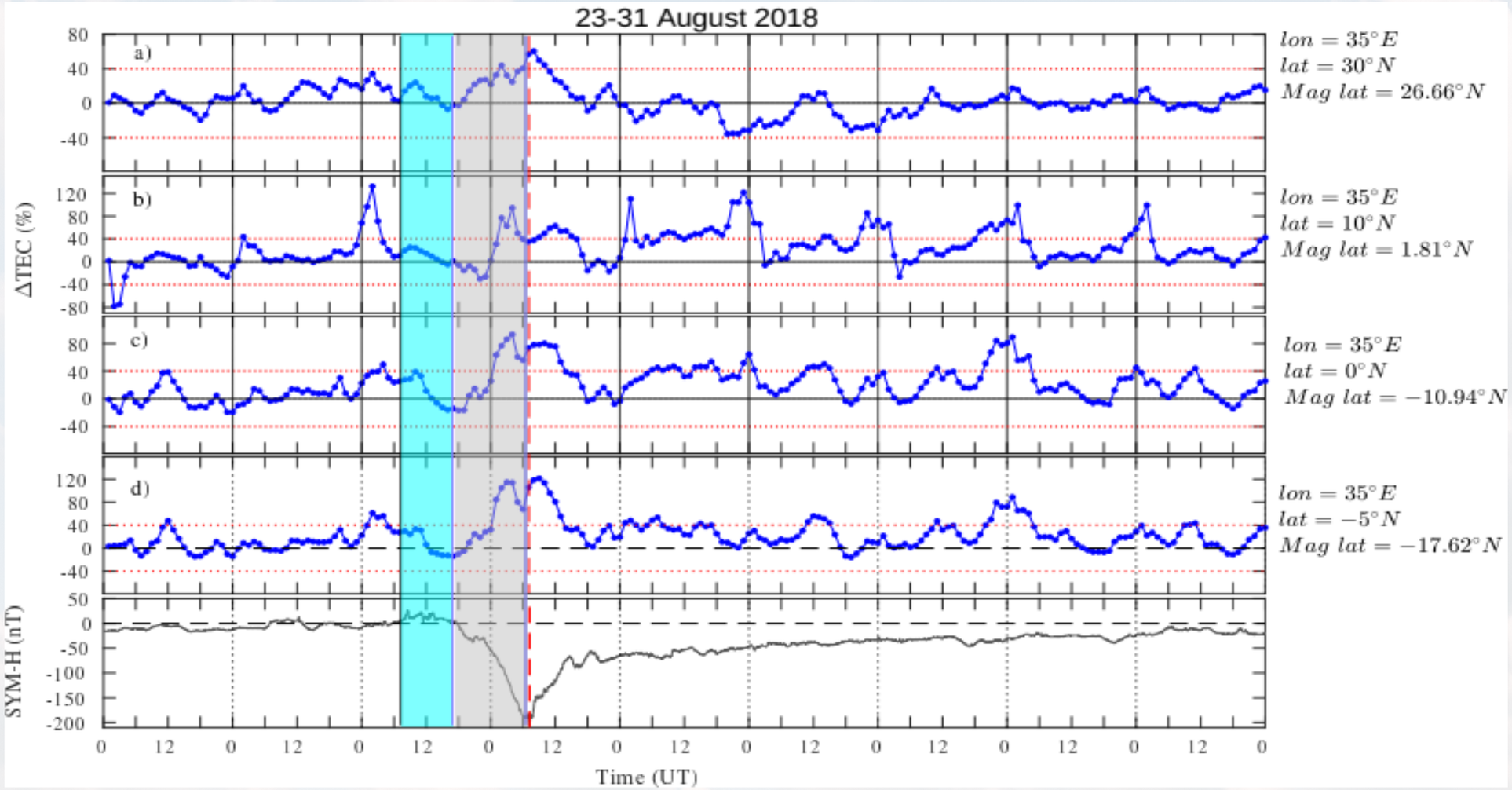

Figure 4: ΔTEC (%) derived from GIM over Europe-African longitude sector (35°E) on different latitudes (mid-latitude, equatorial, and low latitude region) during 23-31 August 2018. **The vertical solid black, magenta, and blue** (red broken line) lines show the beginning of the **initial** (07:45 UT), **main** (17:29 UT), and **recovery** (07:00 UT) phases of the storm, respectively. **The light cyan and gray shaded regions show the initial and main phase of the storm**, respectively (Dugassa et al., 2022).

Ionospheric response: ΔTEC from GPS

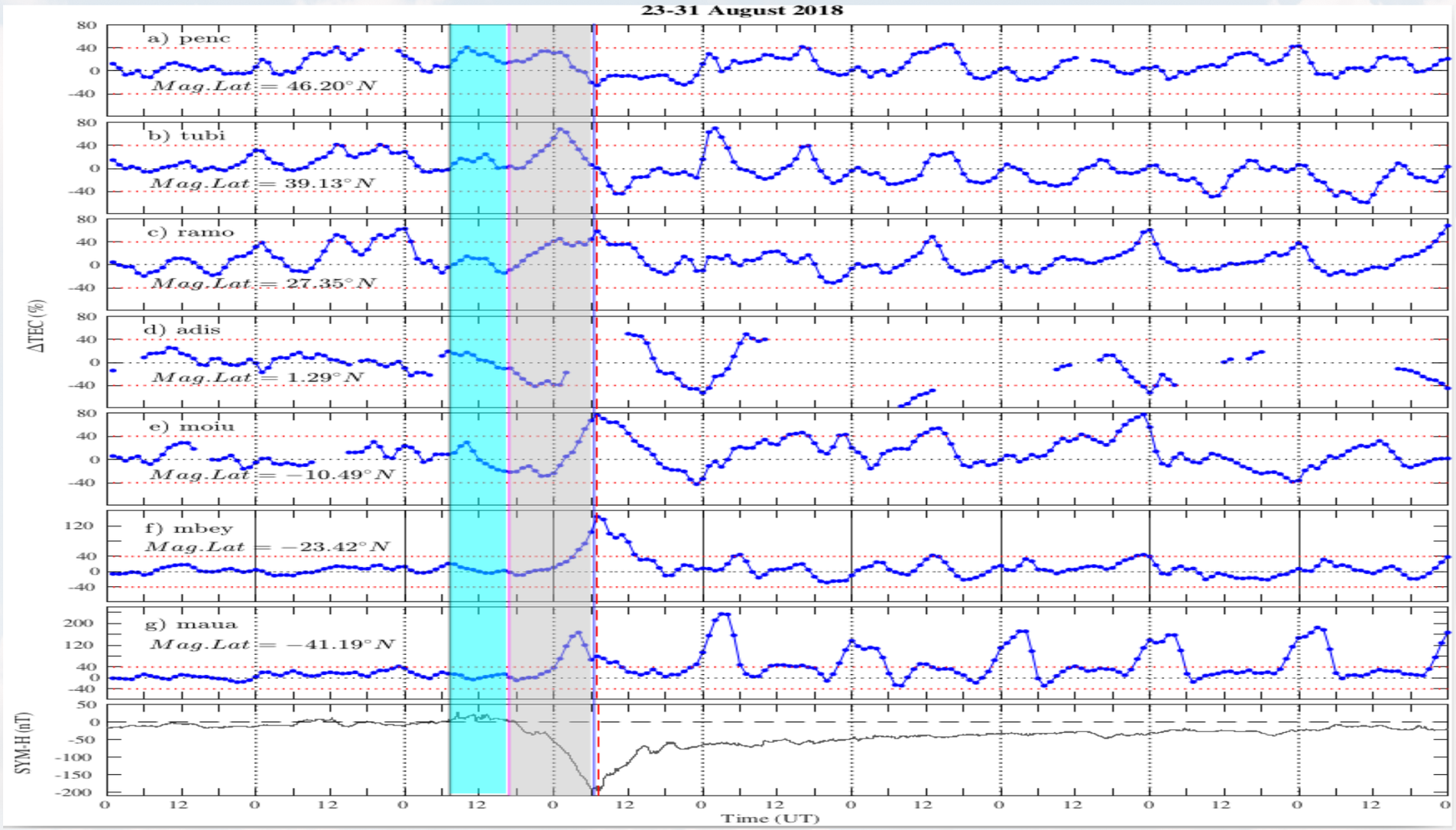

Figure 5: ΔTEC (%) derived from GNSS over Europe-African longitude sector (30±10°E) on different latitudes (mid-latitude, equatorial, and low latitude region) during 23-31 August 2018. The vertical solid black, magenta, and blue (red broken line) lines show the beginning of the initial (07:45 UT), main (17:29 UT), and recovery (07:00 UT) phases of the storm, respectively. The light cyan and gray shaded regions show the initial and main phase of the storm, respectively (Dugassa et al., 2022).

Ionospheric response: Causes

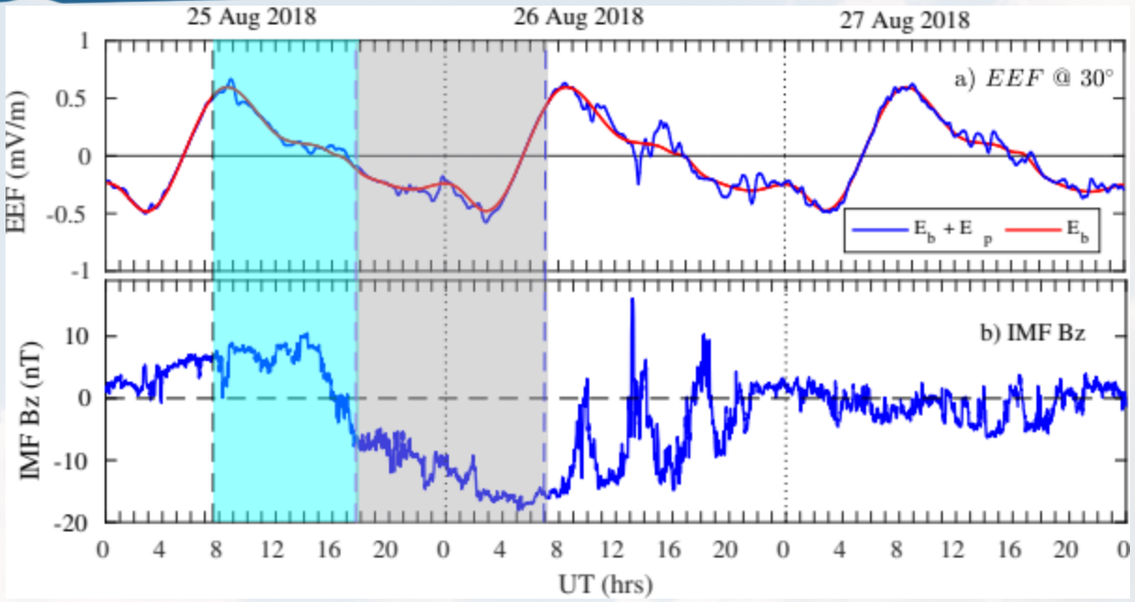

Figure 6: a) The background (red curve) and the combination of the background and the prompt penetration electric field (blue curve) over 30°E
b) z-component of interplanetary magnetic field during 25-27 August 2018. E_b: The background electric field, E_p: The penetration electric field. The light cyan and gray shaded regions show the initial and main phase of the storm, respectively (Dugassa et al., 2022).

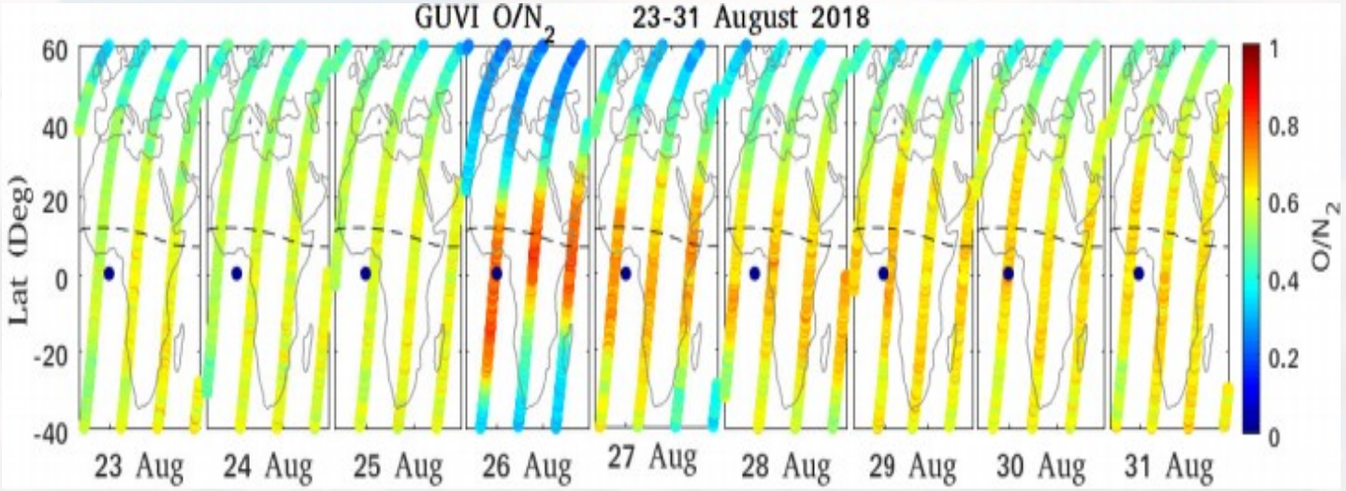

Figure 7: The variation in [O/N_2] ratio obtained from GUVI/TIMED during 23-31 August 2018 over European-African longitude sector. The broken line shows the geomagnetic equator (Dugassa et al., 2022).

Ionospheric irregularities: GPS-ROTI

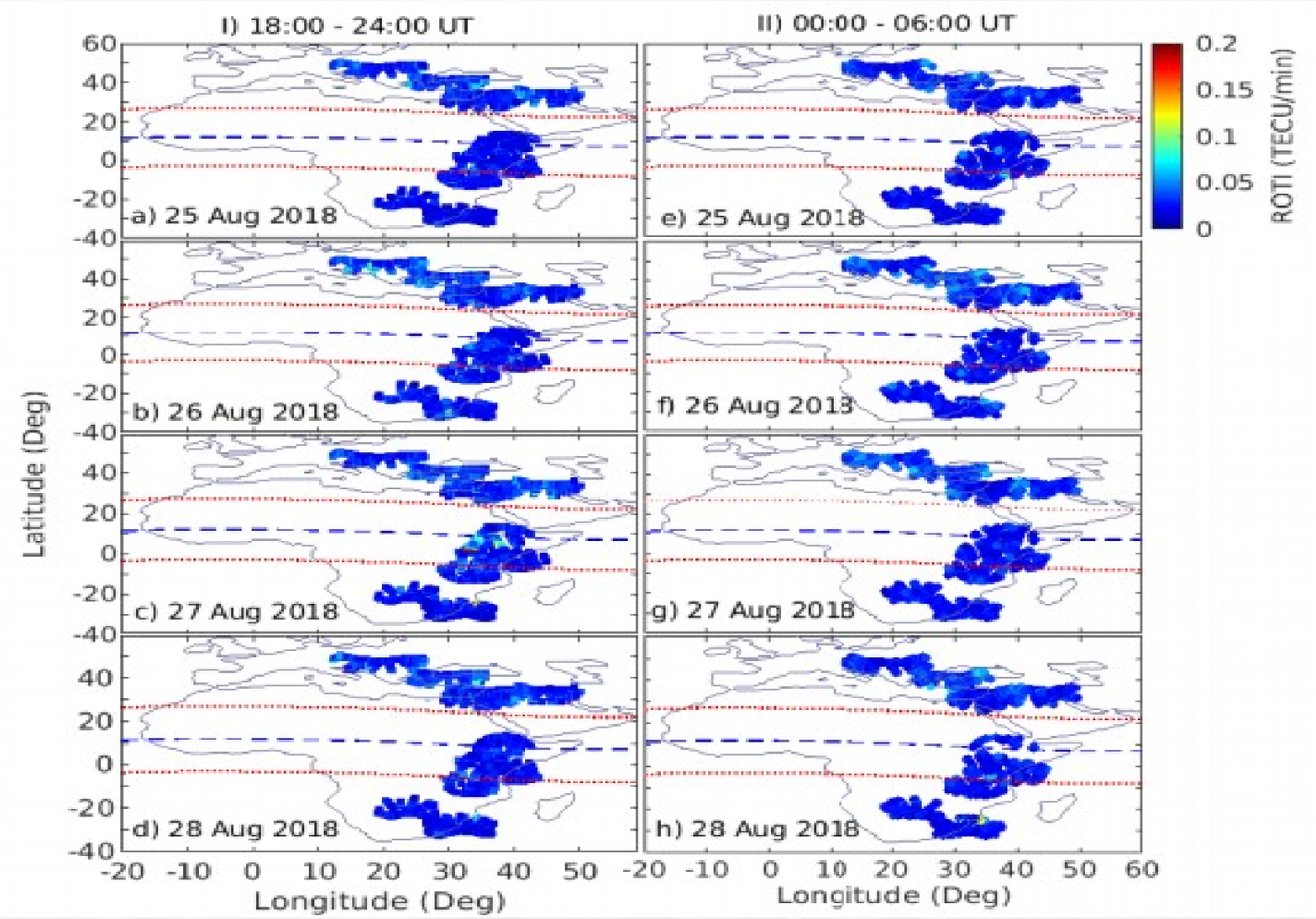

Figure 8: Latitudinal variation of ionospheric irregularities in the I) pre-midnight (18:00–24:00 UT) and II) post-midnight (00:00–06:00 UT) hours over Europe-Africa longitude sector derived from GPS-TEC during 25-28 August 2018. The dot red lines (±15°) and broken blue line (0°) indicate the upper and lower boundaries of low-latitude region and the magnetic equator, respectively (Dugassa et al.,2022).

Ionospheric irregularities: SWARM-RODI

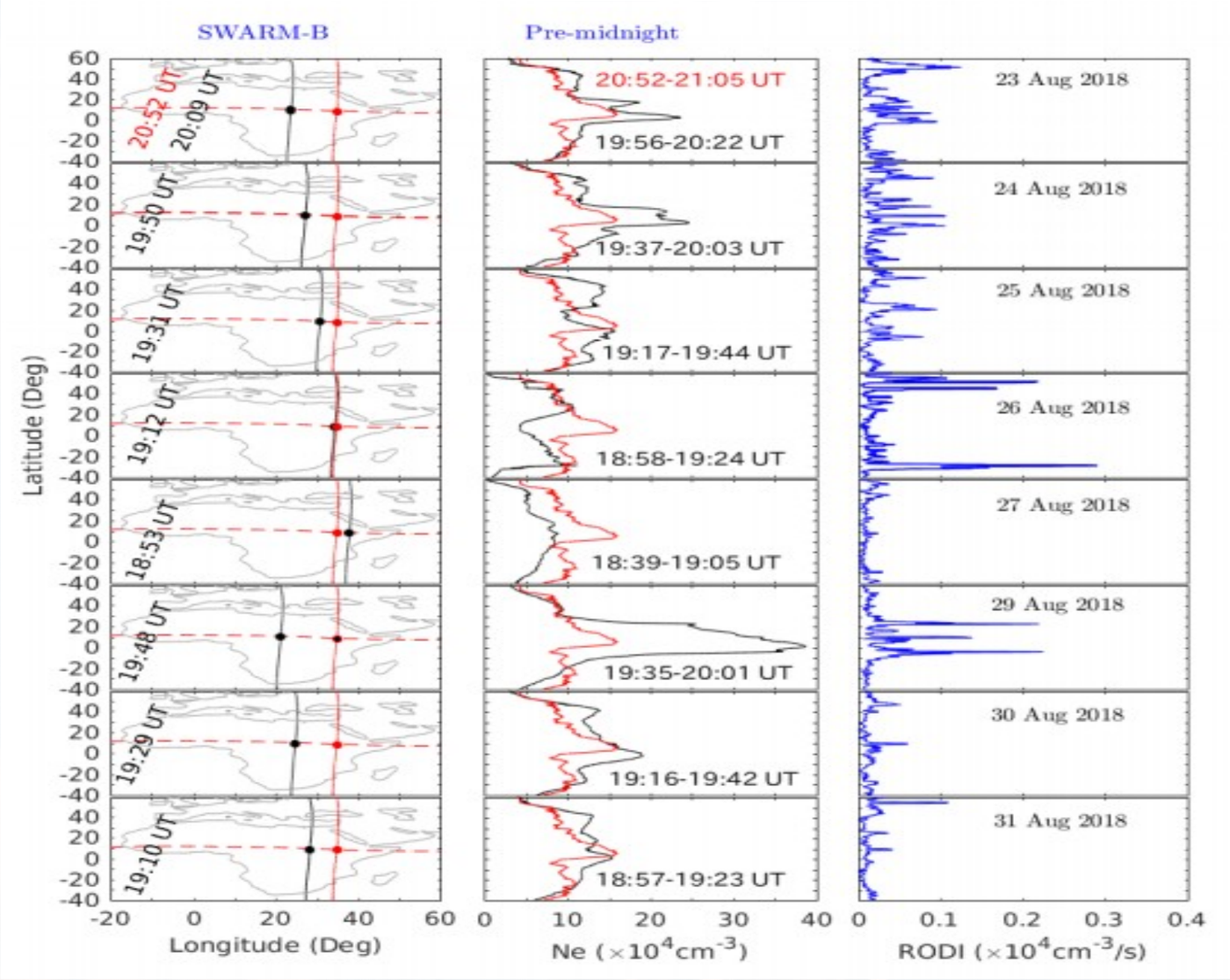

Figure 9: Topside (SWARM-B satellite) pre-midnight observation: (left panels) paths of the satellite, (middle panels) Ionospheric plasma density (Ne), and (right panels) ionospheric plasma density irregularities (RODI, blue curves) during 23-31 August 2018 over Europe-African sector. The red and black curves shows the quiet time (06 August 2018) and observed plasma density (Ne), respectively (Dugassa et al.,2022)..

Ionospheric irregularities: SWARM-RODI

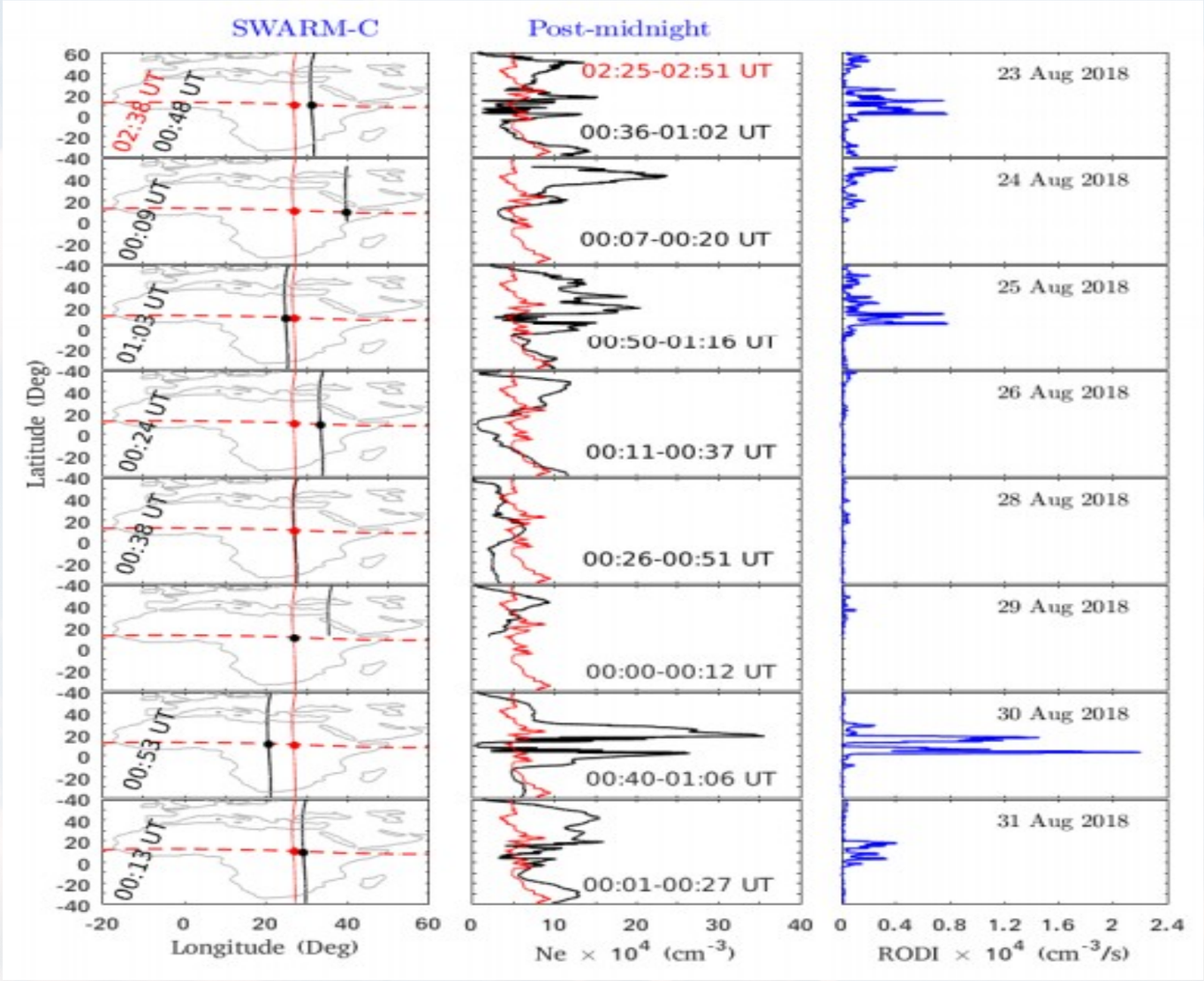

Figure 10: Topside (SWARM-C satellite) Post-midnight observation: (left panels) tracks of the satellite, (middle panels) Ionospheric plasma density (Ne), and (right panels) ionospheric plasma density irregularities (RODI) during 23-26, 28-31 August 2018 over Europe-African sector. The red and black curves shows the quiet time (06 August 2018) and observed plasma density (Ne), respectively (Dugassa et al., 2022).

Conclusion

- Positive ionospheric storm effect in the low-latitude region of Africa, and a negative ionospheric storm effect in the mid-latitude region of Europe and Africa were observed during the storm recovery phase.
- The decrease in [**O/N_2**] ratio is the possible cause for the observed negative ionospheric storm effect.
- Hemispheric asymmetry were noticed over Europe-African longitude sector during the storm main and recovery phases.
- The occurrence of ionospheric irregularities over the low-latitude region of Africa in the premidnight and post-midnight was suppressed (**ROTI<0.4 TECU/min**). This could be related to the local time at which the minimum SYM-H occurred which corresponded to daytime over Europe-African longitude sector.

SSGI

SPACE SCIENCE AND GEOSPATIAL INSTITUTE

FROM EARTH TO SPACE . . .

ከምድር እስከ ህዋ . . .

THANK YOU!